

Step structure on GaAs(113)A studied by scanning tunneling microscopy

L. Geelhaar, J. Márquez, and K. Jacobi*

Fritz-Haber-Institut der Max-Planck-Gesellschaft, Faradayweg 4-6, D-14195 Berlin, Germany

(Received 16 August 1999)

The GaAs(113)A surface was prepared by molecular-beam epitaxy and *in situ* characterized by scanning tunneling microscopy (STM) and low-energy electron diffraction (LEED). The occurrence of an (8×1) reconstruction as proposed by Wassermeier *et al.* [Phys. Rev. B **51**, 14 721 (1995)] was confirmed. Overview STM images reveal a striking anisotropy in the step structure of this surface. While steps along $[3\bar{3}\bar{2}]$ (the $1 \times$ direction of the reconstruction) are straight for up to 2000 Å, steps along $[1\bar{1}0]$ are extremely rough. In this direction, kinks occur typically after less than 100 Å. The ratio of the respective lateral step densities is 8 ± 4 . This anisotropy is explained by applying the electron counting rule (ECR) to one-dimensional islands. While islands along $[3\bar{3}\bar{2}]$ fulfil the ECR, it is violated by islands along $[1\bar{1}0]$. Thus, if structures formed additionally perpendicular to step edges along $[3\bar{3}\bar{2}]$, they would be energetically unfavorable. Hence, growth occurs mainly by propagation along $[3\bar{3}\bar{2}]$. It is suggested that the determining structural element of GaAs(113)A- (8×1) is the zigzag chain of As dimers. [S0163-1829(99)11947-7]

I. INTRODUCTION

Besides reconstruction or relaxation, steps are of particular importance on any surface in that they can act as diffusion barriers and/or incorporation centers for growth. Thus, the microscopic step structure directly influences the surface morphology. Also, for the successful growth of devices a control of the step morphology is essential. On the one hand, flat surfaces with broad terraces and very few steps are desirable for interfaces of heterostructures. On the other hand, a regular array of steps can be used as a substrate for the growth of quantum wires.^{1,2} GaAs(113)A has successfully been employed as a substrate for heterostructures,³⁻⁸ quantum wires⁹ and quantum dots,¹⁰⁻¹⁵ but the bare surface has not been characterized extensively.

In the first studies on GaAs(113)A the surface was prepared by ion-beam annealing (IBA) resulting in (1×1) -low-energy electron diffraction (LEED) images.^{16,17} Nötzel *et al.* reported that on molecular beam epitaxy grown samples a regular array of $\{331\}$ -facets forms,^{18,19} but this finding could not be reproduced by other groups. Instead, based on scanning tunneling microscopy (STM) experiments Wassermeier *et al.*²⁰ proposed an (8×1) -reconstruction (cf. Fig. 1) which was later confirmed by kinematic reflection high-energy electron diffraction (RHEED) simulations,²¹ surface core-level spectroscopy,^{22,23} and total energy calculations using density-functional theory.²⁴ Setzer *et al.* pointed out that actually the reconstruction has to be described by a matrix and that the notation “ (8×1) ” is only correct if a non-primitive unit cell is used,²² but for convenience we will continue to use this short notation. Several authors reported a highly anisotropic surface roughness,^{18-20,25-28} which is not yet understood.

The electron counting rule²⁹⁻³² is a simple rule which helps to determine whether a structural model on a compound semiconductor surface is stable or not. The electron counting rule (ECR) states that all dangling bonds of the cation (e.g., Ga) have to be empty while all dangling bonds

of the anion (e.g., As) have to be completely filled. A structure is said to fulfil the ECR if the electrons contributing to surface bands can be distributed in such a way. So far, on GaAs no reconstruction has been found that violates the ECR. Pashley successfully applied the ECR to islands on GaAs(001)- (2×4) to explain why on this surface steps are smooth in one direction and kinked in the perpendicular direction.³¹ In this paper we will use a similar argumentation to explain the anisotropic step structure on GaAs(113)A- (8×1) .

II. EXPERIMENT

Experiments were carried out in a multi-chamber ultra-high vacuum-system, which is described in detail elsewhere.³³ Samples with a typical size of $10 \times 10 \text{ mm}^2$ were cut from GaAs(113)A wafers (*n*-type, Si-doped, carrier concentration $2.5 \times 10^{18} \text{ cm}^{-3}$, Laser Diode), cleaned with propanole and introduced into the UHV system via a load lock. After oxide desorption samples were treated with several IBA cycles. Layers 20-50 nm thick were grown by MBE at a temperature of 580 °C. The As_2 :Ga beam equivalent pressure ratio was 15. After growth, samples were cooled down to 480 °C while simultaneously the As pressure was reduced. At a base pressure of less than 3×10^{-9} mbar samples were transferred to the analysis chamber. Surfaces were *in situ* studied by STM (Park Scientific Instruments, VP2) and LEED. STM images were acquired in constant current mode with tunneling currents between 0.1 and 1 nA and sample voltages between -2 and -3 V.

III. RESULTS AND DISCUSSION

A. (8×1) reconstruction

The (8×1) periodicity of the reconstruction can clearly be seen in the LEED image shown in Fig. 2. The primitive rhomboedric unit cell of the bulk-truncated surface and the unit cell of the reconstructed surface are indicated. In real

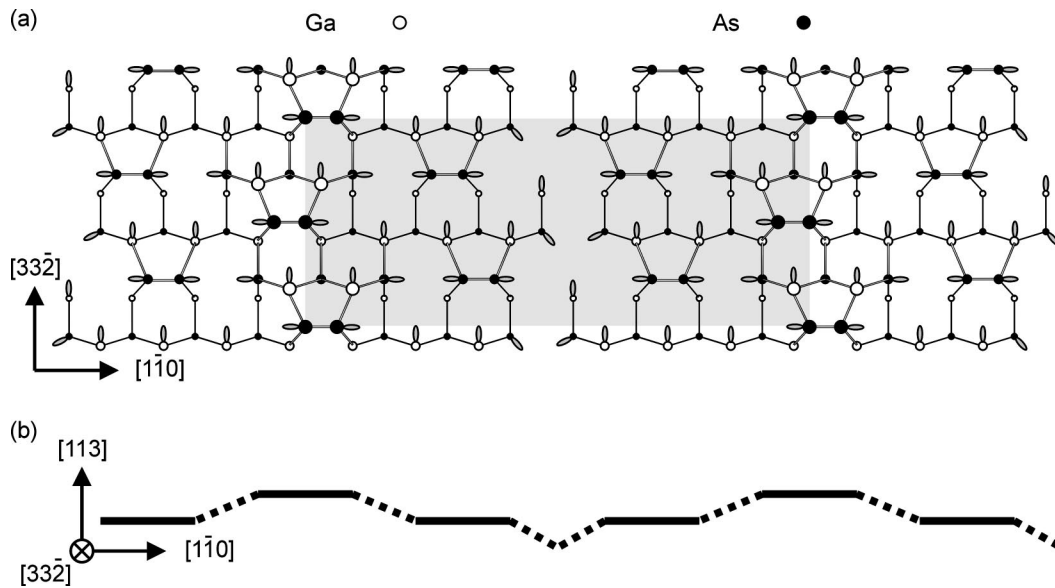


FIG. 1. Structural model of GaAs(113)A-(8×1). (a) Top view. Atoms in the second and in the third layer are depicted by smaller circles. The unit cell is marked by the gray rectangle. (b) Side view. The zigzag chains of As dimers are depicted as horizontal solid lines.

space the length of the latter unit cell is 32.0 Å in the $[1\bar{1}0]$ direction and 13.3 Å in the $[33\bar{2}]$ direction. A structural model of this reconstruction as proposed by Wassermeier *et al.*²⁰ is presented in Fig. 1. Three atomic layers are involved in the reconstruction, thus the corrugation is 3.4 Å. The characteristic element is a zigzag chain of As dimers extending along $[33\bar{2}]$ in the top layer and as well in the middle layer, adjacent but phaseshifted by about a quarter of the length of the unit cell in this direction. Next to the middle layer zigzag chain there is a trench reaching down to the third atomic layer, and on the other side of the trench there are again two zigzag chains, one each in the top and the middle layer. Note that the reconstruction is not symmetrical to the plane through the trench, though. In Fig. 3 a high-resolution STM image of this surface is shown. The bright zigzag lines in the upper right part are the top layer As dimers, and the middle layer As dimers are also visible in between. In the lower-left corner of the image there are two steps downwards to lower layers.

B. Step structure

A larger-area STM image is presented in Fig. 4. Also on this scale, the image is dominated by the chains of As dimers (lines from the upper left to the lower right). The surface roughness is, compared to low-index GaAs surfaces, fairly high and anisotropic, which is typical for this surface.^{20,25–28} However, there are also comparably large flat areas, for example in the upper middle part of Fig. 4. Also, the dimer chains are locally of a high degree of order without any vacancies. Most striking in the image is the anisotropy of the step structure. Step edges along $[33\bar{2}]$ are extremely straight over up to 2000 Å. In contrast, step edges along $[1\bar{1}0]$ are very rough. Only rarely more than three neighboring dimer chains end at the same position. Thus, step edges along $[1\bar{1}0]$ are straight for typically less than 100 Å. In some cases, single dimer chains extend from the step edge by more

than 500 Å (arrow in Fig. 4). In the high-resolution STM image in Fig. 3 it can be seen that step edges along $[33\bar{2}]$ are formed by complete dimer chains as they occur in the (8×1)-unit cell. The step edge parallel to $[1\bar{1}0]$ formed by the end of the dimer chain on the right-hand side of this image is not clearly resolved. Thus, it cannot be concluded if step edges along this direction are also consistent with the reconstruction. Apparently the step structure is determined by the dimer chains characteristic for this reconstruction. A similar anisotropy was observed on GaAs(001)-(2×4) where A-type steps (parallel to the As dimers and along $[1\bar{1}0]$, the 2× direction) are straighter than B-type steps (along $[110]$).^{34,35} The step edges are always formed by complete (2×4) unit cells. The anisotropy can be quantified either by measuring step densities or island lengths along the crystallographic axes, yielding on GaAs(001) ratios A/B ranging from 2 to 10.^{36–41} For this study on GaAs(113)A, six wide scan images on three samples were evaluated by counting the steps

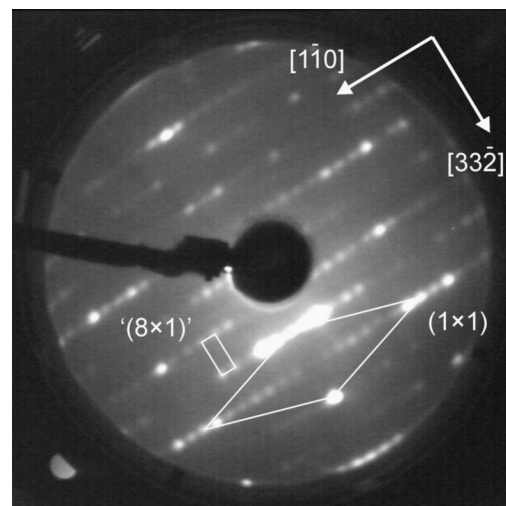


FIG. 2. LEED image of GaAs(113)A-(8×1). $E=55$ eV.

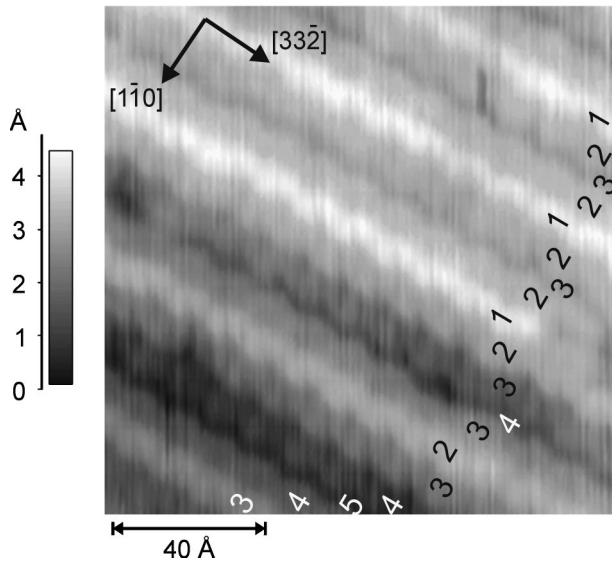


FIG. 3. High-resolution STM image of GaAs(113)A-(8 \times 1). $U_{\text{sample}} = -2.5$ V, $I = 0.3$ nA. The numbers in the image denote the atomic layers, starting from the top layer.

on height profiles along $[1\bar{1}0]$ (giving the lateral step density of steps parallel to $[33\bar{2}]$ and along $[33\bar{2}]$, respectively). Four height profiles were extracted per image and direction. The step density is $(10 \pm 2) \times 10^{-3} \text{ \AA}^{-1}$ for steps parallel to $[33\bar{2}]$ and $(1.3 \pm 0.5) \times 10^{-3} \text{ \AA}^{-1}$ for steps parallel to $[1\bar{1}0]$, and the ratio is 8 ± 4 . The highest ratios on GaAs(001) were found on surfaces that were prepared with special care to reach thermal equilibrium (slow growth rate, long annealing time after growth).^{40,41} No special attention was directed at this point during the experiments presented in this article. Also, the aforementioned high ratios on GaAs(001) were extracted from anisotropic island shapes, thus the length over which step edges are straight without *any* kinks were not measured. In a more detailed analysis the kink lengths and separations were measured and counted.⁴² The highest value reported for kinks in *B*-type steps was four unit cell lengths. In contrast, on GaAs(113)A kinks in steps parallel to $[1\bar{1}0]$ with a length of 25 and more unit cell lengths are not unusual. Therefore, the anisotropy of the step structure is on GaAs(113)A at least as high as on GaAs(001), presumably higher.

Let us now consider one-dimensional islands on the surface in order to understand the anisotropy of the step structure. One-dimensional means here that the islands extend in one direction as little as possible under the constraints of the reconstruction, and infinitely in the perpendicular direction. The structural models were constructed in such a way that all included atoms are, whenever possible, in such a binding configuration as they would be if they were part of the reconstructed surface without an island on top. Downwards directed open bonds were excluded. In the side view of the reconstruction in Fig. 1(b) one can see that, starting from the trench and moving to the right-hand side, the reconstruction consists of two upward steps followed by two downward steps. Instead of going down, one can imagine an additional dimer chain formed after a third step upwards, as depicted in Fig. 5(a) by the dashed line. This way an one-dimensional

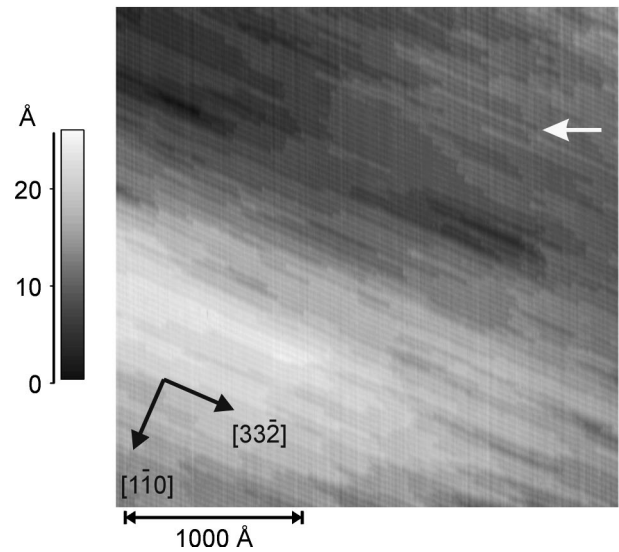


FIG. 4. Overview STM image of GaAs(113)A-(8 \times 1). $U_{\text{sample}} = -2.5$ V, $I = 0.2$ nA.

island along $[33\bar{2}]$ is created. Note that the threefold step upwards can be seen twice in the lower-left part of Fig. 3. There the step leads to a higher layer and not to an island, but the series of three dimer chains is the same. The top view of the island structure described above is shown in Fig. 5(b), where the island is marked by two vertical dashed lines. Although this structure extends in direction $[1\bar{1}0]$ by less than one unit cell length, it is consistent with the (8 \times 1) reconstruction because atoms in new binding configurations do not occur. The connection to the middle layer of the substrate is achieved by (110)-like microfacets with threefold-coordinated Ga and As atoms. The unit cell of the combined structure of an (8 \times 1)-reconstruction with one additional dimer chain on top is shown in Fig. 5(b) by the gray rectangle. Counting of all relevant electrons reveals that this structure fulfils the electron counting rule. Apart from a single dimer chain on top there are other possible one-dimensional islands along $[33\bar{2}]$. Starting from the previous structure, the normal continuation of the (8 \times 1) reconstruction from the dimer chain on top would be a step downwards to a dimer chain *in* the top layer of the substrate, as shown in Fig. 5(c). It is possible to form a link to the substrate by the usual trench element. Another configuration is the one depicted in Fig. 5(d), where the island consists only of the dimer chain added in Fig. 5(c). Finally, a composition of the islands in Figs. 5(a) and 5(c) yields an island whose width is equal to that of a full unit cell of the (8 \times 1) reconstruction [cf. Fig. 5(e)]. There are also equivalent structures that one would get if one started with three upward steps from the right-hand side to the left. All these structures fulfil the electron counting rule.

A model of an one-dimensional island along $[1\bar{1}0]$ is depicted in Fig. 6. Again, the island is marked by two dashed lines and the unit cell by a gray rectangle. Opposed to the situation described in the previous paragraph, in direction $[1\bar{1}0]$ it is not possible to divide the (8 \times 1)-unit cell into smaller elements, like for example dimer chains, without breaking bonds. The model shown in Fig. 6 is the smallest possible island with an (8 \times 1) periodicity. However, even in

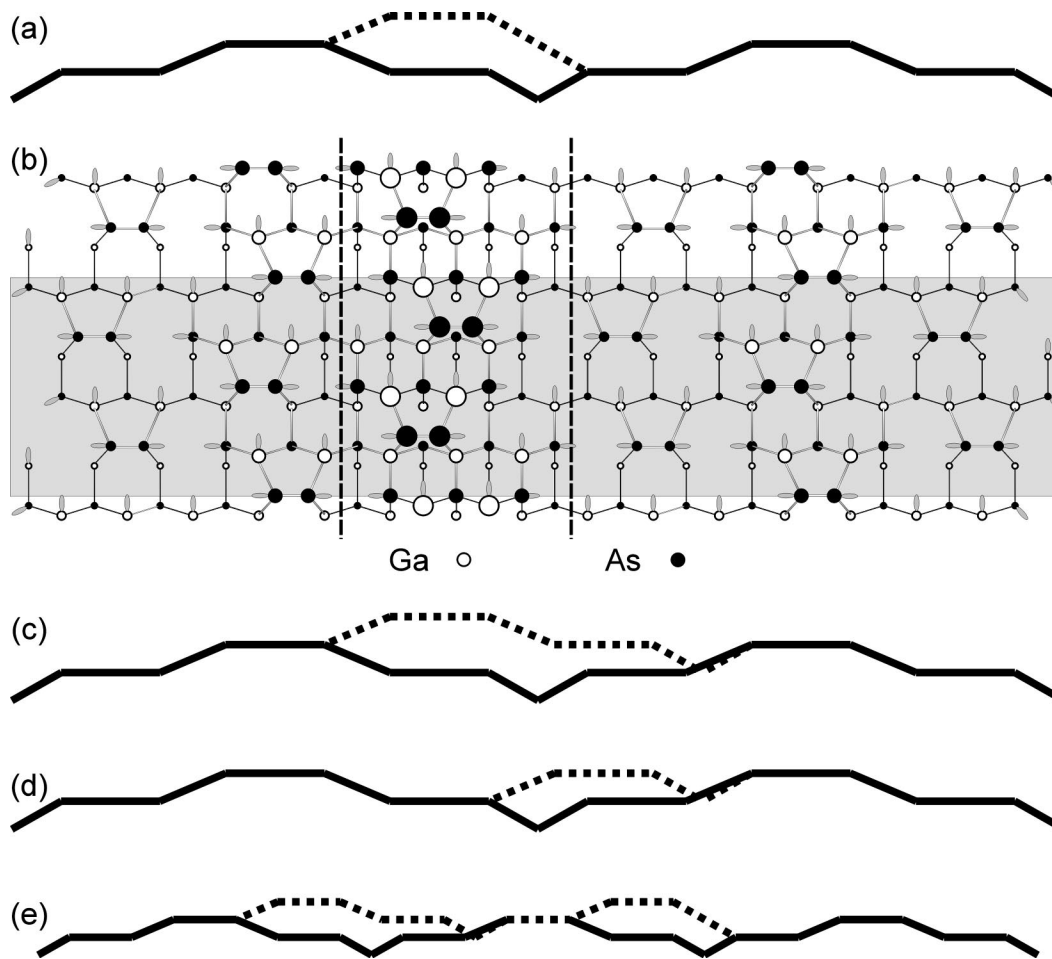


FIG. 5. Models of one-dimensional islands along $[33\bar{2}]$. (a) One dimer chain on top, side view. (b) One dimer chain on top, top view. (c) Two dimer chains, side view. (d) One dimer chain in top layer, side view. (e) Full unit cell width, side view (not in scale).

order to build this island, bonds of the (8×1) reconstruction have to be broken. The dangling bonds created this way are highlighted by a darker shading. Ga atoms with even two dangling bonds occur. Hence, it is not surprising that this structure does not fulfil the electron counting rule. There is one other possible island structure. In the model presented in Fig. 6(a) the part of the dimer zigzag chain added to form the island is within the chain directed from the lower right-hand side to the upper left-hand side (“zig”). If the island is placed on the substrate shifted by half a unit cell in direction $[33\bar{2}]$, the added part of the dimer chain is directed from the lower left-hand side to the upper right-hand side (“zag”). The side view of the island created this way looks the same as in Fig. 6(b). This island contains the same number of each different type of dangling bond and is thus equivalent to the depicted one. Also by putting the additional dimers onto the left-hand side of the substrate top layer equivalent islands are formed. By adding single atoms or dimers we have not been able to find an one-dimensional island along $[1\bar{1}0]$ that fulfils the ECR, either.

The previous considerations enable us now to explain the highly anisotropic step structure on GaAs(113)A- (8×1) . From a step edge along $[1\bar{1}0]$ fingerlike structures can grow into the perpendicular direction without violating the ECR. This is indeed observed in the STM images (cf. arrow in

Fig. 4). Thus, step edges along $[1\bar{1}0]$ are very rough. In contrast, a structure extending from a step edge along $[33\bar{2}]$ would not fulfil the ECR and, thus, would be energetically unfavorable. Hence, step edges along $[33\bar{2}]$ are extremely straight.

The different possible one-dimensional islands in direction $[33\bar{2}]$ along with the STM images imply that the determining structural element of GaAs(113)A is actually not the (8×1) -unit cell but the zigzag chain of As dimers. The step structure of the surface is inherent already in the unit cell, which comprises three atomic layers. This conclusion is supported by a study on InAs(311)A.⁴³ In STM images bright rows running along $[\bar{2}33]$ were observed as on GaAs(311)A- (8×1) and interpreted as As-dimer chains. However, RHEED revealed a (5×1) and a (15×2) periodicity, depending on preparation conditions. The authors concluded that there are the same As-dimer chains on the surface as on GaAs(113)A- (8×1) , but in a different arrangement resulting in a different unit cell.

Our findings also suggest that growth on GaAs(113)A- (8×1) takes place mostly by propagation along $[33\bar{2}]$. The same was reported on InAs(311)A based on a strong azimuthal dependence of RHEED oscillations.⁴³ A careful inspection of the structural model shown in Fig. 6 makes growth by incorporation at step edges parallel to

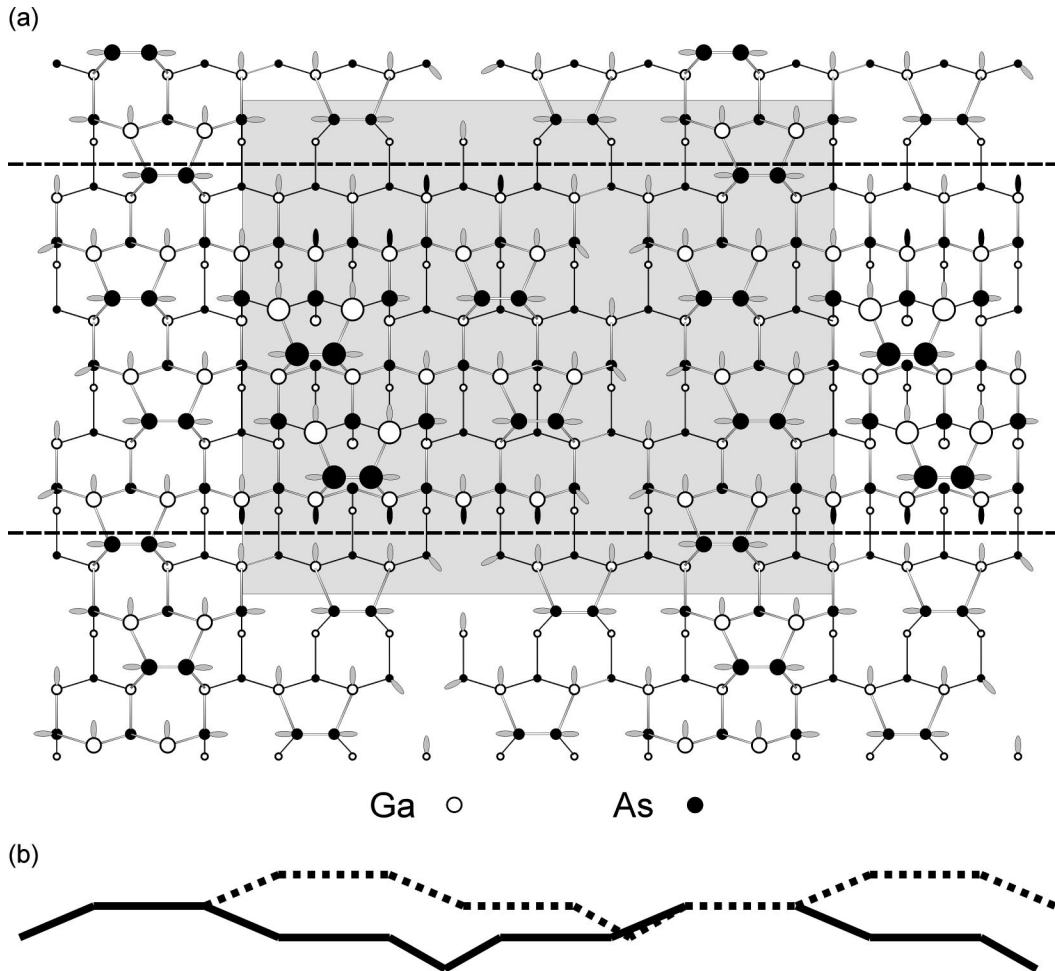


FIG. 6. Model of a one-dimensional island along $[1\bar{1}0]$. (a) Top view. (b) Side view.

$[1\bar{1}0]$ plausible. The formation of this step always yields more dangling bonds than on the reconstructed terraces, thus species diffusing on the surface can easily find binding sites. In contrast, at step edges parallel to $[33\bar{2}]$ [cf. Fig. 5(b)] there is the same number of dangling bonds in the same configuration as on terraces.

There are three possible causes for the anisotropic step structure: different step energies, different step reactivities, and anisotropic diffusion on the surface. In this paper, we have addressed the first two points. The results of applying the electron counting rule suggest that the energy of steps along $[33\bar{2}]$ is lower than the one of steps in the perpendicular direction. The occurrence of new dangling bonds in the structural model presented in Fig. 6 makes plausible that the incorporation probability is higher at step edges parallel to $[1\bar{1}0]$. Thus, these two factors affect the step morphology in the same direction. An evaluation of the influence of diffusion is not possible on the basis of our results. Diffusion on GaAs(113)A was examined by Pristovsek *et al.*,²⁸ but a possible anisotropy was not considered.

IV. CONCLUSIONS

The step structure of GaAs(113)A- (8×1) exhibits a striking anisotropy. While step edges along $[33\bar{2}]$ are ex-

remely smooth, step edges along $[1\bar{1}0]$ are very rough. This finding can be explained by applying the electron counting rule to one-dimensional islands on this surface. Islands along $[1\bar{1}0]$ violate the ECR, thus structures protruding from step edges along $[33\bar{2}]$ would be energetically unfavorable. In contrast, islands along $[33\bar{2}]$ fulfil the ECR, and fingerlike structures extending from step edges along $[1\bar{1}0]$ are seen in the STM images. Our findings suggest that the determining structural element of this surface is the zigzag chain of As dimers and that this must be energetically very favorable. Also, it is suspected that growth occurs mainly by propagation along $[33\bar{2}]$.

ACKNOWLEDGMENTS

We would like to thank Peter Geng for technical assistance. This work was supported by the Deutsche Forschungsgemeinschaft (Sonderforschungsbereich 296, Project A2) and by the German Bundesministerium für Bildung und Forschung under Grant No. 05 622 EBA4.

- *Corresponding author. Electronic address: jacobi@fhi-berlin.mpg.de, phone: +49-30-8413 5201, fax: +49-30-8413 5106.
- ¹S. Hasegawa, M. Sato, K. Maehashi, H. Asahi, and H. Nakashima, *J. Cryst. Growth* **111**, 371 (1991).
 - ²S. Hara, J. Motohisa, T. Fukui, and H. Hasegawa, *Jpn. J. Appl. Phys., Part 1* **34**, 4401 (1995).
 - ³W. I. Wang, E. E. Mendez, Y. Iye, B. Lee, M. H. Kim, and G. E. Stillman, *J. Appl. Phys.* **60**, 1834 (1986).
 - ⁴O. Brandt, K. Kanamoto, Y. Tokuda, N. Tsukada, O. Wada, and J. Tanimura, *Phys. Rev. B* **48**, 17 599 (1993).
 - ⁵G. Armelles, P. Castrillo, P. S. Dominguez, L. González, A. Ruiz, D. A. Contreras-Solorio, V. R. Velasco, and F. García-Moliner, *Phys. Rev. B* **49**, 14 020 (1994).
 - ⁶Y. Hsu, W. I. Wang, and T. S. Kuan, *Phys. Rev. B* **50**, 4973 (1994).
 - ⁷Y. Hsu, W. I. Wang, and T. S. Kuan, *J. Vac. Sci. Technol. B* **14**, 2286 (1996).
 - ⁸S. Ghosh, B. M. Arora, S.-J. Kim, J.-H. Noh, and H. Asahi, *J. Appl. Phys.* **85**, 2687 (1999).
 - ⁹R. Nötzel, J. Menninger, M. Ramsteiner, A. Ruiz, H.-P. Schönherr, and K. H. Ploog, *Appl. Phys. Lett.* **68**, 1132 (1996).
 - ¹⁰P. O. Vaccaro, M. Hirai, K. Fujita, and T. Watanabe, *J. Phys. D* **29**, 2221 (1996).
 - ¹¹M. Henini, S. Sanguinetti, L. Brusaferrri, E. Grilli, M. Guzzi, M. D. Upward, P. Moriarty, and P. H. Beton, *Microelectron. J.* **28**, 933 (1997).
 - ¹²S. T. Stoddart, A. Polimeni, M. Henini, L. Eaves, P. C. Main, R. K. Hayden, K. Uchida, and N. Miura, *Appl. Surf. Sci.* **123/124**, 366 (1998).
 - ¹³S. C. Fortina, S. Sanguinetti, E. Grilli, M. Guzzi, M. Henini, A. Polimeni, and L. Eaves, *J. Cryst. Growth* **187**, 126 (1998).
 - ¹⁴M. Henini, S. Sanguinetti, S. C. Fortina, E. Grilli, M. Guzzi, G. Panzarini, L. C. Andreani, M. D. Upward, P. Moriarty, P. H. Beton, and L. Eaves, *Phys. Rev. B* **57**, R6815 (1998).
 - ¹⁵R. Nötzel, Z. Niu, M. Ramsteiner, H.-P. Schönherr, A. Tranpert, L. Däweritz, and K. H. Ploog, *Nature (London)* **392**, 56 (1998).
 - ¹⁶K. Stiles and A. Kahn, *J. Vac. Sci. Technol. B* **3**, 1089 (1985).
 - ¹⁷L. Ö. Olsson, M. Björkqvist, J. Kanski, L. Ilver, and P. O. Nilsson, *Surf. Sci.* **366**, 121 (1996).
 - ¹⁸R. Nötzel, N. N. Ledentsov, L. Däweritz, M. Hohenstein, and K. Ploog, *Phys. Rev. Lett.* **67**, 3812 (1991).
 - ¹⁹R. Nötzel, N. N. Ledentsov, L. Däweritz, K. Ploog, and M. Hohenstein, *Phys. Rev. B* **45**, 3507 (1992).
 - ²⁰M. Wassermeier, J. Sudijono, M. D. Johnson, K. T. Leung, B. G. Orr, L. Däweritz, and K. Ploog, *Phys. Rev. B* **51**, 14 721 (1995).
 - ²¹W. Braun, O. Brandt, M. Wassermeier, L. Däweritz, and K. Ploog, *Appl. Surf. Sci.* **104/105**, 35 (1996).
 - ²²C. Setzer, J. Platen, P. Geng, W. Ranke, and K. Jacobi, *Surf. Sci.* **377-379**, 125 (1997).
 - ²³C. Setzer, J. Platen, W. Ranke, and K. Jacobi, *Surf. Sci.* **419**, 291 (1999).
 - ²⁴J. Platen, A. Kley, C. Setzer, K. Jacobi, P. Ruggerone, and M. Scheffler, *J. Appl. Phys.* **85**, 3597 (1999).
 - ²⁵R. Nötzel, J. Temmyo, and T. Tamamura, *Appl. Phys. Lett.* **64**, 3557 (1994).
 - ²⁶M. Pristovsek, H. Menhal, T. Wehnert, J.-T. Zettler, T. Schmidting, N. Esser, W. Richter, C. Setzer, J. Platen, and K. Jacobi, *J. Cryst. Growth* **195**, 1 (1998).
 - ²⁷M. Pristovsek, H. Menhal, T. Schmidting, N. Esser, and W. Richter, *Microelectron. J.* **30**, 449 (1999).
 - ²⁸M. Pristovsek, H. Menhal, J.-T. Zettler, and W. Richter, *Appl. Surf. Sci.* (in press).
 - ²⁹J. A. Appelbaum, G. A. Baraff, and D. R. Hamann, *Phys. Rev. B* **14**, 1623 (1976).
 - ³⁰W. A. Harrison, *J. Vac. Sci. Technol.* **16**, 1492 (1979).
 - ³¹M. D. Pashley, *Phys. Rev. B* **40**, 10 481 (1989).
 - ³²D. J. Chadi, in *Springer Series in Surface Sciences*, Vol. 24, edited by S. Y. Tong, M. A. Van Hove, K. Takayanagi, and X. D. Xie (Springer-Verlag, Berlin, Heidelberg, 1991), p. 532.
 - ³³P. Geng, J. Márquez, L. Geelhaar, J. Platen, C. Setzer, and K. Jacobi, *Rev. Sci. Instrum.* (in press).
 - ³⁴P. R. Pukite, G. S. Petrich, S. Batra, and P. I. Cohen, *J. Cryst. Growth* **95**, 269 (1989).
 - ³⁵M. D. Pashley, K. W. Haberern, and J. M. Gaines, *Appl. Phys. Lett.* **58**, 406 (1991).
 - ³⁶G. R. Bell, M. Itoh, T. S. Jones, and B. A. Joyce, *Surf. Sci.* **423**, L280 (1999).
 - ³⁷J. Kim, M. C. Gallagher, R. F. Willis, J. Fu, and D. L. Miller, *J. Vac. Sci. Technol. B* **11**, 1370 (1993).
 - ³⁸V. Bressler-Hill, R. Maboudian, M. Wassermeier, X.-S. Wang, K. Pond, P. M. Petroff, and W. H. Weinberg, *Surf. Sci.* **287/288**, 514 (1993).
 - ³⁹K. Pond, R. Maboudian, V. Bressler-Hill, D. Leonard, X.-S. Wang, K. Self, W. H. Weinberg, and P. M. Petroff, *J. Vac. Sci. Technol. B* **11**, 1374 (1993).
 - ⁴⁰T. Ide, A. Jamashita, and T. Mizutani, *Phys. Rev. B* **46**, 1905 (1992).
 - ⁴¹E. J. Heller and M. G. Lagally, *Appl. Phys. Lett.* **60**, 2675 (1992).
 - ⁴²E. J. Heller, Z. Y. Zhang, and M. G. Lagally, *Phys. Rev. Lett.* **71**, 743 (1993).
 - ⁴³D. I. Lubyshev, M. Micovic, D. L. Miller, I. Chizhov, and R. F. Willis, *J. Vac. Sci. Technol. B* **16**, 1339 (1998).